Aging and confinement in subordinated fractional Brownian motion

Yingjie Liang [1,2,*] Wei Wang,[2,†] and Ralf Metzler [2,3,‡]
[1]*College of Mechanics and Engineering Science, Hohai University, 211100 Nanjing, China*
[2]*Institute of Physics & Astronomy, University of Potsdam, 14476 Potsdam, Germany*
[3]*Asia Pacific Centre for Theoretical Physics, Pohang 37673, Republic of Korea*

(Received 31 January 2024; revised 27 May 2024; accepted 29 May 2024; published 20 June 2024)

We study the effects of aging properties of subordinated fractional Brownian motion (FBM) with drift and in harmonic confinement, when the measurement of the stochastic process starts a time $t_a > 0$ after its original initiation at $t = 0$. Specifically, we consider the aged versions of the ensemble mean-squared displacement (MSD) and the time-averaged MSD (TAMSD), along with the aging factor. Our results are favorably compared with simulations results. The aging subordinated FBM exhibits a disparity between MSD and TAMSD and is thus weakly nonergodic, while strong aging is shown to effect a convergence of the MSD and TAMSD. The information on the aging factor with respect to the lag time exhibits an identical form to the aging behavior of subdiffusive continuous-time random walks (CTRW). The statistical properties of the MSD and TAMSD for the confined subordinated FBM are also derived. At long times, the MSD in the harmonic potential has a stationary value, that depends on the Hurst index of the parental (nonequilibrium) FBM. The TAMSD of confined subordinated FBM does not relax to a stationary value but increases sublinearly with lag time, analogously to confined CTRW. Specifically, short aging times t_a in confined subordinated FBM do not affect the aged MSD, while for long aging times the aged MSD has a power-law increase and is identical to the aged TAMSD.

DOI: 10.1103/PhysRevE.109.064144

I. INTRODUCTION

Anomalous diffusion processes have been widely observed in diverse systems of physics, chemistry, biology, and hydrogeology [1–12], featuring a power law form

$$\langle x^2(t)\rangle = 2D_\rho t^\rho \tag{1}$$

of the mean-squared displacement (MSD), where the generalized diffusion coefficient has physical dimension $[D_\rho] = \text{length}^2/\text{time}^\rho$, and the anomalous diffusion exponent distinguishes the regimes of subdiffusion with $0 < \rho < 1$ and superdiffusion with $\rho > 1$, including the special cases of Brownian motion with $\rho = 1$ and ballistic diffusion with $\rho = 2$ [13–15]. *Inter alia*, subdiffusion was observed for the passive motion of submicron tracers in living biological cells [16–19], of lipids and proteins in membranes [20–24], bacteria in biofilms [25], or water diffusion in rat brain tissues [26]. Superdiffusion fueled by molecular motors was observed for virus motion in cells [27], messenger ribonucleoproteins in neuronal cells [28], vacuoles in amoeba cells [29], amoeba cells themselves [30,31], in mussel colonies [32], tracer dispersion in aquifers [33,34], or for water absorption in swelling soil [35].

Anomalous diffusion may emerge from a variety of physical stochastic processes, including the famed continuous-time random walk (CTRW) and fractional Brownian motion (FBM). The CTRW model introduced by Montroll and Weiss [36] generalizes a random walk in such a way that the particle waits for a random time between jumps. When the mean waiting time diverges, subdiffusion emerges, and the anomalous diffusion exponent ρ equals the scaling exponent α of the waiting-time probability density function (PDF) $\psi(t) \simeq t^{-1-\alpha}$. Such subdiffusive CTRW was found in highly heterogeneous media such as amorphous semiconductors [37], live cell membranes [24], glass-forming liquids [38], and sand columns [39]. Power-law waiting times were discussed in the context of transmission errors in telephone circuits by Berger and Mandelbrot in 1963 [40]. CTRWs with power-law waiting times were considered by Montroll and Scher in 1973 [41], see also the work by Shlesinger [42]. For more details we refer to the review by Bouchaud and Georges [43] and the book by Hughes [44]. The FBM model originally devised by Kolmogorov [45] and further developed by Mandelbrot and van Ness [46], is a non-Markovian process driven by zero-mean, stationary Gaussian noise with long-range correlations. FBM has been applied to describe anomalous diffusion in complex liquids [47,48], living cells [49], brain fibers [50], and financial markets [51]. In a comparative study dissecting the observed motion in terms of the Mandelbrot scaling exponents, a diverse range of processes, from molecular diffusion to the motion of larger animals such as storks or vultures, long-range dependencies, were detected [52,53].

There exist a growing number of data from single-particle tracking studies [54–58] indicating that the observed motion corresponds to a stochastic process featuring more than a single generating mechanism. Therefore, compound processes with more multifaceted statistical characteristics are required. In particular, we here mention systems in which CTRW and FBM exist simultaneously. These include the motion of

*Contact author: liangyj@hhu.edu.cn
†Contact author: weiwangnuaa@gmail.com
‡Contact author: rmetzler@uni-potsdam.de

insulin granules in living MIN6 insulisoma cells [59], of nicotinic acetylcholine membrane receptors [60], nanosized tracer objects in the cytoplasm [10], drug molecules confined by silica slabs [58], and of voltage-gated sodium channels on the surface of hippocampal neurons [61]. A process combining FBM and CTRW was recently studied [61] in terms of a subordination concept [62–64], i.e., FBM subordinated via a stable subordinator. In our previous work, the statistical properties of this stochastic process with an external drift were studied, revealing features of non-Gaussianity and nonergodicity [65]. Here we address the question on the aging properties and confinement of such a process.

Particular focus in our study will be put on aging properties. Aging in the sense pursued here is the response to the observed dynamics to a time delay between the original initiation of the physical process at $t = 0$ and the start of the observation at some time $t_a > 0$. Aging is a key property of glassy systems [66] but was also rationalized in polymeric semiconductors [67], living MIN6 insulisoma cells [59], the surface of hippocampal neurons [61], groundwater systems [33,34], and quantum dots [68]. The CTRW model is an aging process [69], contrasting the nonaging of FBM [15]. Here we will analyze the aging properties of subordinated FBM. Apart from free motion and motion in the presence of a drift, we here also consider the motion in a harmonic potential. Pure FBM and CTRW in an external harmonic potential were studied previously [70–79]. In particular, it was shown that the ensemble MSD and time-averaged MSD (TAMSD) for confined FBM initially grows as a free FBM and reaches a stationary plateau at long times [70]. The ensemble MSD of confined subdiffusive CTRW initially grows as a free CTRW and reaches a plateau at long times; in contrast to FBM, however, the behavior of the TAMSD is different: instead of reaching a plateau it continues to grow as a power law with scaling exponent $1 - \alpha$ [73,78]. We here investigate analytically and numerically the statistical properties of aging subordinated FBM with drift and confined in a harmonic potential.

This paper is organized as follows. In Sec. II, subordinated FBM with drift and its properties are introduced. Section III focuses on the aging effects on MSD, TAMSD, and the aging factor of subordinated FBM. Section IV investigates the statistical properties of MSD and TAMSD of confined subordinated FBM. Finally, in Sec. V we conclude.

II. SUBORDINATED FBM WITH DRIFT

We start with a primer on the main properties of subordinated FBM with drift in the absence of aging [61,65]. Subordination here means that a process defined in terms of the operational time s is then transformed to the process in real time t, i.e., $x(t) \equiv x(s(t))$, in terms of the coupled stochastic Langevin equations [80–84]

$$\frac{dx(s)}{ds} = v + \sqrt{2D}\zeta_H(s), \quad \frac{dt(s)}{ds} = \varepsilon(s), \tag{2}$$

where v, if different from zero, is the constant drift velocity. Without loss of generality we set $D = 1/2$. $\zeta_H(s)$ is the so-called fractional Gaussian noise with zero mean, defined by its correlation function for $t_1 \neq t_2$,

$$\langle \zeta_H(t_1)\zeta_H(t_2)\rangle \sim H(2H-1)|t_1 - t_2|^{2H-2}. \tag{3}$$

Here H denotes the Hurst exponent $0 < H < 1$. For pure FBM the Hurst exponent H gives rise to the ensemble MSD Eq. (1) with $\rho = 2H$.

$\varepsilon(s)$ is the one-sided Lévy stable noise [85], which is the formal derivative of the Lévy stable subordinator $t(s)$ with stability index $0 < \alpha \leqslant 1$. The Lévy stable subordinator is a nondecreasing Lévy process with stationary and independent increments. The one-sided Lévy stable distribution is defined in terms of its Laplace transform [86]

$$\hat{L}_\alpha^+(p) = \int_0^\infty L_\alpha^+(t)\exp(-pt)dt = \exp(-p^\alpha). \tag{4}$$

The inverse subordinator $s(t)$ is defined as $s(t) = \inf\{s > 0 : t(s) > t\}$ and is called the hitting time or first-passage time process [87], which can be considered as the limit process of the CTRW with a heavy-tailed waiting time PDF. The inverse subordinator $s(t)$ is responsible for the subdiffusive behavior with long rests of the particle and the parental process $x(s)$ above introduces FBM with drift. Both of $x(s)$ and $s(t)$ determine the properties of subordinated FBM.

The moments $\langle x^n(t)\rangle$ of $x(t)$ defined in Eq. (2) are [86]

$$\langle x^n(t)\rangle = \int_0^\infty \langle x^n(s)\rangle h(s,t)ds, \tag{5}$$

where $\langle x^n(s)\rangle$ represent the moments of the parental FBM process, and the PDF of the inverse stable subordinator $s(t)$ reads

$$h(s,t) = \frac{t}{\alpha s^{1+1/\alpha}} L_\alpha^+\left(\frac{t}{s^{1/\alpha}}\right), \tag{6}$$

in terms of the one-sided Lévy stable distribution L_α^+. For the general distribution L_α^+ in Eq. (6) the first and second moments were obtained in the form [65]

$$\langle x(t)\rangle = \frac{v}{\Gamma(1+\alpha)}t^\alpha \tag{7}$$

and

$$\langle x^2(t)\rangle = \frac{\Gamma(1+2H)}{\Gamma(1+2H\alpha)}t^{2H\alpha} + \frac{2v^2}{\Gamma(1+2\alpha)}t^{2\alpha}. \tag{8}$$

The MSD of the subordinated process is then given by

$$\langle \Delta x^2(t)\rangle = \frac{\Gamma(1+2H)}{\Gamma(1+2H\alpha)}t^{2H\alpha} + \left(\frac{2}{\Gamma(1+2\alpha)} - \frac{1}{\Gamma(1+\alpha)^2}\right)v^2 t^{2\alpha}, \tag{9}$$

in which the drift term does not cancel out and will asymptotically dominate. We note that for $1/2 < \alpha < 1$ this dominant behavior is superdiffusive, a finding known from biased subdiffusive CTRWs [37,88]. Intuitively, this behavior is a consequence of the fast transport of mobile particles, separating rapidly from the particles still trapped at the origin. In contrast to biased Brownian motion for which the relative particle spread becomes ever sharper, $\sqrt{\langle \Delta x^2(t)\rangle}/\langle x(t)\rangle \simeq t^{-1/2}$ [37,88], in subdiffusive CTRW this quantity converges to a constant, i.e., the process remains smeared out—effecting the power-law shape of the first-passage times [89]. In our case here we see that for $\alpha = 1$ the ballistic term in the MSD Eq. (9) vanishes and, similarly, $\sqrt{\langle \Delta x^2(t)\rangle}/\langle x(t)\rangle \simeq t^{H-1}$ decays as function of time.

The TAMSD is defined as [4,15]

$$\overline{\delta^2(\Delta)} = \frac{1}{T-\Delta}\int_0^{T-\Delta}[x(t+\Delta)-x(t)]^2 dt, \tag{10}$$

where T is referred to as the measurement time (length of the time series) and Δ is called the lag time which defines the width of the window slid along the time series $x(t)$. The TAMSD is thus the appropriate statistical observable to evaluate single-particle trajectories [4] when only few but long trajectories are available from experiment. Ergodicity is here understood in the Boltzmann-Khinchin-Birkhoff sense that for sufficiently long trajectories the magnitudes of the MSD and the TAMSD in the limit $\Delta/T \to 0$ are identical [13,15,73].

For subordinated FBM [65], the explicit increment reads

$$\begin{aligned}\langle[x(t+\Delta)-x(t)]^2\rangle &= \frac{2v^2}{\Gamma(\alpha)\Gamma(2+\alpha)}\,{}_2F_1\left(1,1-\alpha;2+\alpha;-\frac{\Delta}{t}\right)\frac{\Delta^{1+\alpha}}{t^{1-\alpha}}\\ &\quad+\frac{\Gamma(1+2H)}{\Gamma(\alpha)\Gamma(2-\alpha+2H\alpha)}\\ &\quad\times {}_2F_1\left(1,1-\alpha;2-\alpha+2H\alpha;-\frac{\Delta}{t}\right)\frac{\Delta^{1-\alpha+2H\alpha}}{t^{1-\alpha}}.\end{aligned} \tag{11}$$

Here ${}_2F_1$ denotes the hypergeometric function [90]. In the limit of short lag times $\Delta/T \ll 1$, the TAMSD becomes [65]

$$\begin{aligned}\langle\overline{\delta^2(\Delta)}\rangle &\sim \frac{2v^2}{\alpha\Gamma(\alpha)\Gamma(2+\alpha)}\frac{\Delta^{1+\alpha}}{T^{1-\alpha}}\\ &\quad+\frac{\Gamma(1+2H)}{\alpha\Gamma(\alpha)\Gamma(2-\alpha+2H\alpha)}\frac{\Delta^{1-\alpha+2H\alpha}}{T^{1-\alpha}}.\end{aligned} \tag{12}$$

The disparity between the TAMSD and the ensemble MSD reflects the weak ergodicity breaking caused by the diverging waiting-time scale in subdiffusive CTRW [15,91].

III. AGING EFFECTS IN SUBORDINATED FBM WITH DRIFT

We now turn to the effects of aging, when the observation starts a time $t_a > 0$ after the system initiation. Without limiting generality we use the convention that the system is prepared at $t = 0$.

A. Mean-squared displacement

The aging MSD in subordinated FBM can be derived in the form [92,93]

$$\begin{aligned}\left\langle x_a^2(t_a,t)\right\rangle &= \langle[x(t_a+t)-x(t_a)]^2\rangle\\ &= \frac{2v^2}{\Gamma(\alpha)\Gamma(2+\alpha)}\,{}_2F_1\left(1,1-\alpha;2+\alpha;-\frac{t}{t_a}\right)\frac{t^{1+\alpha}}{t_a^{1-\alpha}}\\ &\quad+\frac{\Gamma(1+2H)}{\Gamma(\alpha)\Gamma(2-\alpha+2H\alpha)}\\ &\quad\times {}_2F_1\left(1,1-\alpha;2-\alpha+2H\alpha;-\frac{t}{t_a}\right)\frac{t^{1-\alpha+2H\alpha}}{t_a^{1-\alpha}}.\end{aligned} \tag{13}$$

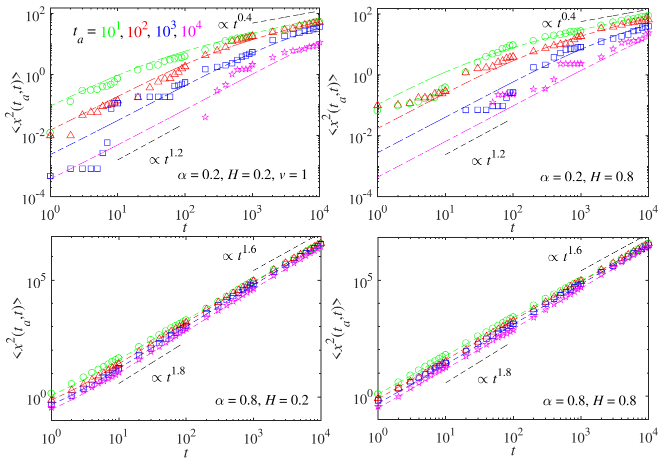

FIG. 1. MSD for aged subordinated FBM with drift $v = 1$ and different values of the Hurst exponent H and the waiting-time scaling exponent α. The data points with the corresponding color correspond to different aging times t_a. The dashed curves in the same colors represent Eq. (13), and the dashed black curves of the asymptotic forms $t^{1+\alpha}$ are derived from Eq. (14), while $t^{2\alpha}$ is derived from Eq. (15). Parameters: trajectory lengths $T = 10^4$, elementary time-step $dt = 0.1$, and number of trajectories $n = 300$.

When aging is pronounced, $t \ll t_a$, the aging MSD takes on the limiting form

$$\begin{aligned}\left\langle x_a^2(t_a,t)\right\rangle &\sim \frac{2v^2}{\Gamma(\alpha)\Gamma(2+\alpha)}\frac{t^{1+\alpha}}{t_a^{1-\alpha}}\\ &\quad+\frac{\Gamma(1+2H)}{\Gamma(\alpha)\Gamma(2-\alpha+2H\alpha)}\frac{t^{1-\alpha+2H\alpha}}{t_a^{1-\alpha}}.\end{aligned} \tag{14}$$

When $\alpha = 1$, both expressions (13) and (14) reduce to the nonaging MSD Eq. (8). This case $\alpha = 1$ with finite characteristic waiting time, as expected, does not exhibit any aging effects, analogous to standard FBM [75,93,94] or Brownian motion when $H = 1/2$ [91].

In the opposite case $t \gg t_a$, the aged MSD is

$$\begin{aligned}\left\langle x_a^2(t_a,t)\right\rangle &\sim \frac{2v^2}{\Gamma(1+2\alpha)}[t^{2\alpha}+(\alpha-1)t_a t^{2\alpha-1}]\\ &\quad+\frac{\Gamma(1+2H)}{\Gamma(1+2H\alpha)}[t^{2H\alpha}+(\alpha-1)t_a t^{2H\alpha-1}].\end{aligned} \tag{15}$$

Thus, when the aging time t_a is small as compared to the process time t, the ensemble MSD Eq. (15) is the same as the nonaged MSD in Eq. (8).

Figure 1 shows the analytical results along with stochastic simulations of the aged MSD with drift $v = 1$ for the Hurst exponents $H = 0.2$ and $H = 0.8$, and for the waiting-time scaling exponents $\alpha = 0.2$ and $\alpha = 0.8$. The analytical results are in nice agreement with the simulations. In particular, for progressively longer aging times t_a the crossover from the aging-controlled scaling $t^{1+\alpha}$ to the anomalous scaling $t^{2\alpha}$ is nicely visible in the aged MSD with drift.

In Fig. 2 we depict the results of our analytical calculations and stochastic simulations of the aged MSD without drift. The values of the aged MSD grow faster with time for aged subordinated FBM with drift as compared to the same motion

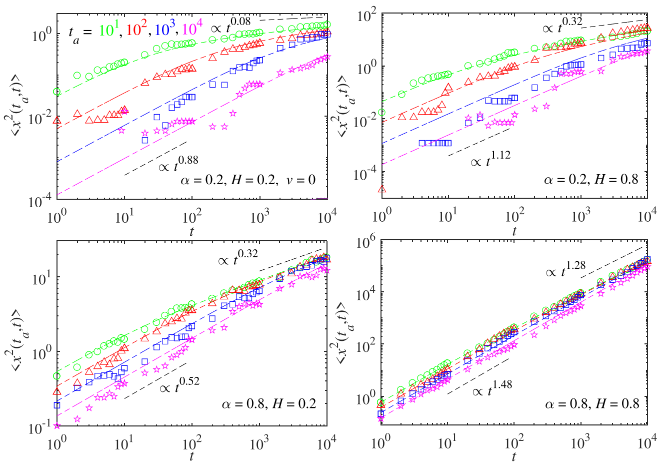

FIG. 2. MSD for aged subordinated FBM without drift $v = 0$. The dashed curves in the same colors represent Eq. (13), while the dashed black curves of the asymptotic forms $t^{1-\alpha+2H\alpha}$ are derived from Eq. (14), $t^{2H\alpha}$ from Eq. (15). Other parameters as in Fig. 1 (in this and all other plots of the main text, if not specified otherwise).

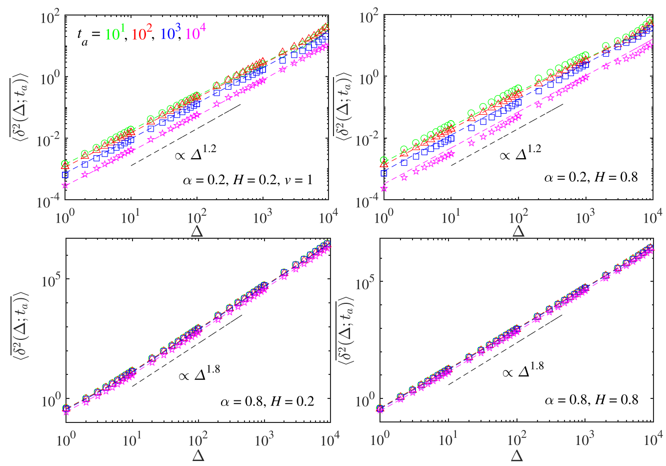

FIG. 3. TAMSD for aged subordinated FBM with drift $v = 1$. The colored dashed curves represent Eq. (18), and the dashed black curves show the asymptotic form $\Delta^{1+\alpha}$ derived from Eq. (18).

in absence of the drift. For longer aging times t_a the crossover from the aging-controlled anomalous scaling $t^{1-\alpha+2H\alpha}$ to the anomalous scaling $t^{2H\alpha}$ is clearly observed in the aged MSD without drift.

B. Time-averaged mean-squared displacement

The aged TAMSD is defined as

$$\overline{\delta^2(\Delta;t_a)} = \frac{1}{T-\Delta}\int_{t_a}^{t_a+T-\Delta}[x(t+\Delta)-x(t)]^2 dt, \tag{16}$$

where, as before, T is the measurement time and Δ is the time lag.

Following the above physical measurement scenario, the mean of the aged TAMSD

$$\langle\overline{\delta^2(\Delta;t_a)}\rangle = \frac{1}{N}\sum_{i=1}^{N}\overline{\delta_i^2(\Delta;t_a)} \tag{17}$$

over N trajectories labeled with the index i, for $\Delta \ll T$ can be derived as

$$\begin{aligned}\langle\overline{\delta^2(\Delta;t_a)}\rangle \sim{}& \frac{2v^2}{\alpha\Gamma(\alpha)\Gamma(2+\alpha)}\Delta^{1+\alpha}\frac{(t_a+T)^\alpha - t_a^\alpha}{T}\\ &+\frac{\Gamma(1+2H)}{\alpha\Gamma(\alpha)\Gamma(2-\alpha+2H\alpha)}\Delta^{1-\alpha+2H\alpha}\\ &\times\frac{(t_a+T)^\alpha - t_a^\alpha}{T}.\end{aligned} \tag{18}$$

When $t_a \ll T$ we recover the known result given in Eq. (12) in the absence of aging. In the limit $t_a \gg T$ of strong aging, the TAMSD in Eq. (18) reduces to the form

$$\begin{aligned}\langle\overline{\delta^2(\Delta;t_a)}\rangle \sim{}& \frac{2v^2}{\Gamma(\alpha)\Gamma(2+\alpha)}\frac{\Delta^{1+\alpha}}{t_a^{1-\alpha}}\\ &+\frac{\Gamma(1+2H)}{\Gamma(\alpha)\Gamma(2-\alpha+2H\alpha)}\frac{\Delta^{1-\alpha+2H\alpha}}{t_a^{1-\alpha}}.\end{aligned} \tag{19}$$

In the limit of strong aging, the aged TAMSD is equivalent to the aged MSD Eq. (14), and thus ergodicity is restored, as already observed for aging CTRW [93] and aging-scaled Brownian motion [95]. This can be understood because in this limit, when measurement time T is much shorter than the aging time t_a, the increments in the TAMSD Eq. (16), $x(t+\Delta)-x(t), t \in [t_a, t_a+T-\Delta]$ change only marginally and are almost identical to $x(t_a+\Delta)-x(t_a)$. However, we note that due to its nonstationary nature the system still explicitly depends on the aging time t_a even in the limit when t_a tends to infinity.

Figure 3 shows the results of our analytical calculations and stochastic simulations of the aged TAMSD with drift $v = 1$. The simulated aged TAMSD reveals good agreement with the analytical form Eq. (18). The anomalous scaling $\simeq \Delta^{1+\alpha}$ is accurately captured.

In Fig. 4 we present the results of our analytical calculations and stochastic simulations of the aged MSD without drift. The values of the aged TAMSD grow much faster with

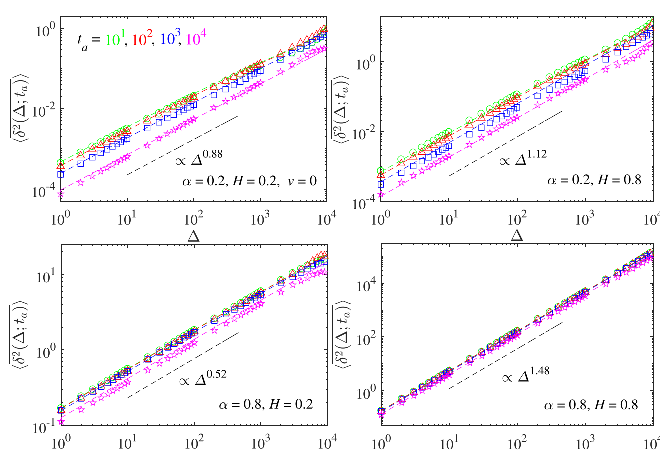

FIG. 4. TAMSD for aged subordinated FBM without drift, $v = 0$. The colored dashed represent Eq. (18), the dashed black curves show the asymptotic form $\Delta^{1-\alpha+2H\alpha}$ derived from Eq. (18).

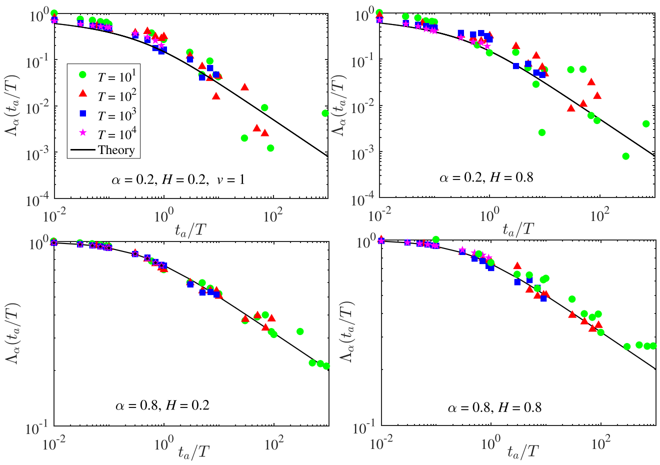

FIG. 5. Aging factor for aged subordinated FBM with drift $v = 1$ and for different measurement times T. The solid dark curves represent Eq. (20).

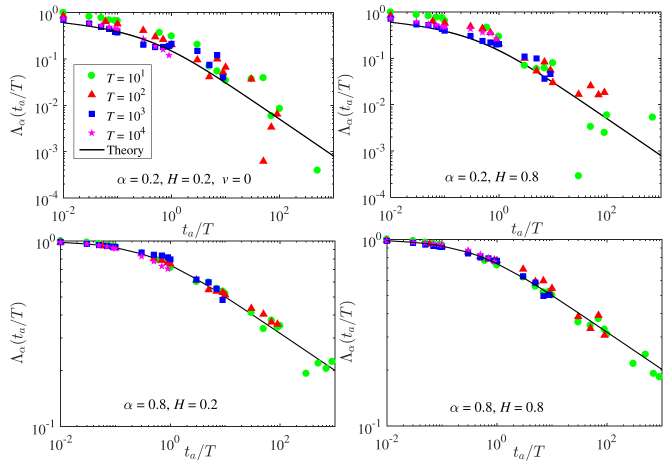

FIG. 6. Aging factor for aged subordinated FBM without drift $v = 0$ and different measurement times T. The solid dark curves represent Eq. (20).

time for aged subordinated FBM with drift as compared to the same motion in absence of the drift. The anomalous scaling $\simeq \Delta^{1-\alpha+2H\alpha}$ is nicely visible.

C. Aging factor

The aging factor $\Lambda(t_a/T)$ describes the ratio of the aged versus the nonaged TAMSDs [92,93]. Based on Eq. (18), the aging factor follows the asymptotic form

$$\Lambda(t_a/T) = \frac{\langle\overline{\delta^2(\Delta;t_a)}\rangle}{\langle\overline{\delta^2(\Delta;t_a=0)}\rangle} \sim (1+t_a/T)^\alpha - (t_a/T)^\alpha. \quad (20)$$

We find that this result is the same as that for pure subdiffusive CTRW motion [92,93], as expected. Note that the same form is also obtained for other anomalous diffusion processes, such as scaled Brownian motion [95] or heterogeneous diffusion processes [96]. Here we conclude that subordinated FBM inherits the aging properties from the scale-free CTRW process. In the nonaging limit, we see that $\Lambda(0) = 1$, and in the limit of very strong aging, $\lim_{z\to\infty} \Lambda(z) = 0$. It emerges that the particles move into areas with low diffusivity, in which they will encounter more and more long waiting times during the aging period. Such scenarios may be found in amorphous semiconductors or groundwater tracer motion [69,97], or for cement fluidity studies with different ages [98].

Figures 5 and 6, respectively, show the results of analytical calculations and stochastic simulations of the aging factor for subordinated FBM with drift $v = 1$ and without drift $v = 0$. The agreement of the simulations with Eq. (20) is good, particularly for cases with larger values of α.

IV. CONFINED SUBORDINATED FBM

We finally turn to confined subordinated FBM in an external harmonic potential of the form $U(x) = kx^2/2$, where k is the stiffness of the trap. This causes a linear restoring force on the process $x(s)$. The corresponding coupled Langevin equations read

$$\frac{dx(s)}{ds} = -kx(s) + \zeta_H(s), \quad \frac{dt(s)}{ds} = \varepsilon(s). \quad (21)$$

For the initial condition $x(0) = 0$, the MSD of the parental FBM process in operational time s is [70]

$$\langle x^2(s)\rangle = \frac{\gamma(2H+1,ks)}{2k^{2H}} + s^{2H}e^{-ks} - \frac{k}{4H+2}s^{2H+1}e^{-2ks} \times M(2H+1, 2H+2, ks), \quad (22)$$

where $\gamma(x, y)$ is the lower incomplete Gamma function [99]

$$\gamma(x,y) = \int_0^y u^{x-1}e^{-u}du, \quad (23)$$

and $M(x, y, z)$ is the Kummer function of the first kind [100],

$$M(x,y,z) = \frac{\Gamma(y)}{\Gamma(x)\Gamma(y-x)}\int_0^1 e^{zu}u^{x-1}(1-u)^{y-x-1}du. \quad (24)$$

The MSD $\langle x^2(t)\rangle$ of the subordinated process then follows from application of Eq. (5). This MSD can be calculated numerically. For the special case $H = 1/2$, the MSD can be explicitly calculated as [78]

$$\langle x^2(t)\rangle = \frac{1}{2k} - \frac{1}{2k}E_\alpha(-2kt^\alpha), \quad (25)$$

where $E_\alpha(-z) = \sum_{i=0}^{\infty}(-z)^i/\Gamma(1+\alpha i)$ is the Mittag-Leffler function [101]. At short times the MSD for arbitrary H coincides with free-subordinated FBM as given in Eq. (8) with $v = 0$, and at long times it arrives at the stationary value

$$\langle x^2(t)\rangle_{\rm st} \sim \frac{\Gamma(2H+1)}{2k^{2H}}. \quad (26)$$

We note that this value is independent of α. This is due to the fact that subdiffusive CTRWs relax towards the equilibrium Boltzmann density in confinement [13,77]. FBM, in contrast, is a nonequilibrium process driven by external noise [102] and therefore $\langle x^2(t)\rangle_{\rm st}$ explicitly depends on H [103].

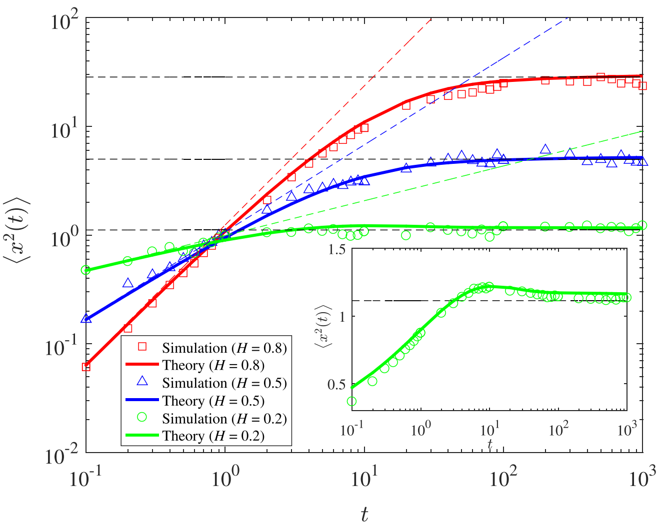

FIG. 7. MSD for confined subordinated FBM. The colored solid curves represent Eq. (5) with Eqs. (6) and (22). The colored dashed curves are from Eq. (8), and the dashed black lines are from Eq. (26). Inset: enlargement of the MSD for $H = 0.2$. Parameters: $k = 0.1$, $\alpha = 0.8$, trajectory lengths $T = 10^3$, elementary time-step $dt = 0.1$, and number of trajectories $n = 300$.

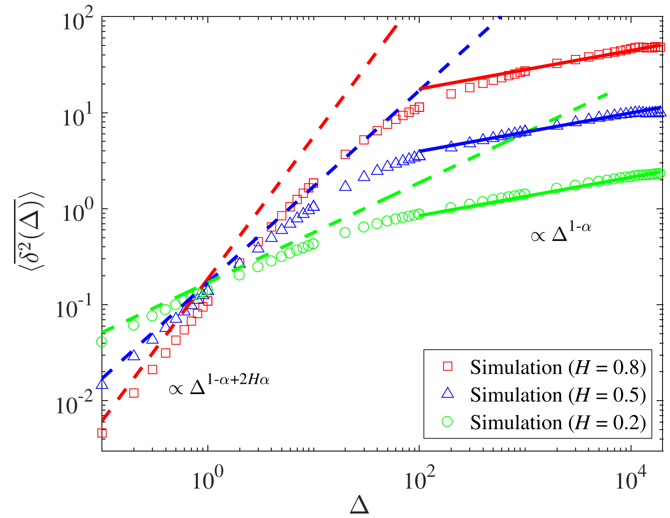

FIG. 8. TAMSD for confined subordinated FBM. The colored dashed curves represent Eq. (12) with $v = 0$, the colored solid curves are from Eq. (27). Parameters: $k = 0.1$, $\alpha = 0.8$, length of trajectories $T = 2 \times 10^4$, elementary time-step $dt = 0.1$, and number of trajectories $n = 300$.

Figure 7 shows the results of our analytical calculations and stochastic simulations of the MSD for confined subordinated FBM with the Hurst exponents $H = 0.2$, $H = 0.5$, and $H = 0.8$, and for the waiting-time scaling exponent $\alpha = 0.8$. The analytical results are in nice agreement with the simulations. At short times $t \ll k^{-1/\alpha}$ the MSD is the same as that of free-subordinated FBM as given by Eq. (8), while at long times $t \gg k^{-1/\alpha}$ (independent of H) it saturated to the stationary value given by Eq. (26). In particular for $H = 0.2$, the subdiffusive particle overshoots before a decrease back to the stationary value (see inset in Fig. 7). This interesting feature of the relaxation dynamics on intermediate time scales was also found for confined pure FBM [70,75,76].

To calculate the TAMSD for confined subordinated FBM, we follow the strategy based on the autocorrelation function given in our previous work [65]. At short times the TAMSD is the same as the one for free-subordinated FBM as given in Eq. (12) with $v = 0$. Different from the asymptotic plateau of the MSD, at long lag times $\Delta \gg k^{-1/\alpha}$ the TAMSD of confined subordinated FBM is sublinearly dependent on lag time Δ:

$$\langle\overline{\delta^2(\Delta)}\rangle_{\rm st} \sim \frac{\Gamma(2H+1)}{k^{2H}}\frac{\sin(\alpha\pi)}{\alpha(1-\alpha)\pi}\left(\frac{\Delta}{T}\right)^{1-\alpha}. \tag{27}$$

This is a direct extension of the behavior of confined subdiffusive CTRWs [73,93,104].

Figure 8 shows the results of stochastic simulations of the TAMSD for confined subordinated FBM with the Hurst exponents $H = 0.2$, $H = 0.5$, and $H = 0.8$, along with the waiting-time scaling exponent $\alpha = 0.8$. At short times the behavior is the same as the one for free-subordinated FBM as given by Eq. (12), while it increases sublinearly with lag time as given by Eq. (27). This contrasts the stationary state of confined FBM attained at long times. Note, however, that even for FBM there exists a nonergodic behavior in the relaxation to the plateau: the ensemble MSD has an exponential relaxation, while it is a slower power law for the TAMSD [48,70].

Figure 9 shows the aged MSD and TAMSD of confined subordinated FBM. For $t_a \ll k^{-1/\alpha}$, the aging time t_a has no effect on the aged MSD and we find the approximation [Fig. 9(a)]

$$\left\langle x_a^2(t_a,\Delta)\right\rangle \approx \langle x^2(\Delta)\rangle, \tag{28}$$

while for $t_a \gg k^{-1/\alpha}$, the aged MSD shows a monotonic increase with the power-law scaling $\Delta^{1-\alpha}$ and is identical to the aged TAMSD [see in Fig. 9(b)]

$$\left\langle x_a^2(t_a,\Delta)\right\rangle = \langle\overline{\delta^2(\Delta;t_a)}\rangle. \tag{29}$$

Concurrently, from aging renewal theory [93] we find that the aged TAMSD for $T \gg \Delta$ can be rewritten as

$$\langle\overline{\delta^2(\Delta;t_a)}\rangle = \langle\overline{\delta^2(\Delta)}\rangle \times \Lambda(t_a/T) \tag{30}$$

valid for all t_a. The aging factor $\Lambda(t_a/T)$ is given by expression (20). Ergodicity is thus restored from Eq. (30) due to the fact that the confined subordinated FBM process arrives at the stationary state when t_a becomes very large and thus the increment $x(t_a + \Delta) - x(t_a)$ solely depends on the lag time Δ.

V. CONCLUSIONS

We studied theoretically and numerically the aging behavior of subordinated FBM. We paid specific emphasis on the comparisons between the cases with and without drift for aging subordinated FBM. When an external drift is present the aging effects are Hurst exponent-independent at long times for both aged MSD and aged TAMSD. The aging factor is also Hurst exponent independent both with and without drift, which is similar to that of aged subdiffusive CTRW. In the strong aging cases, the ergodicity is restored (equivalence of MSD and TAMSD), while it is nonergodic for weak aging.

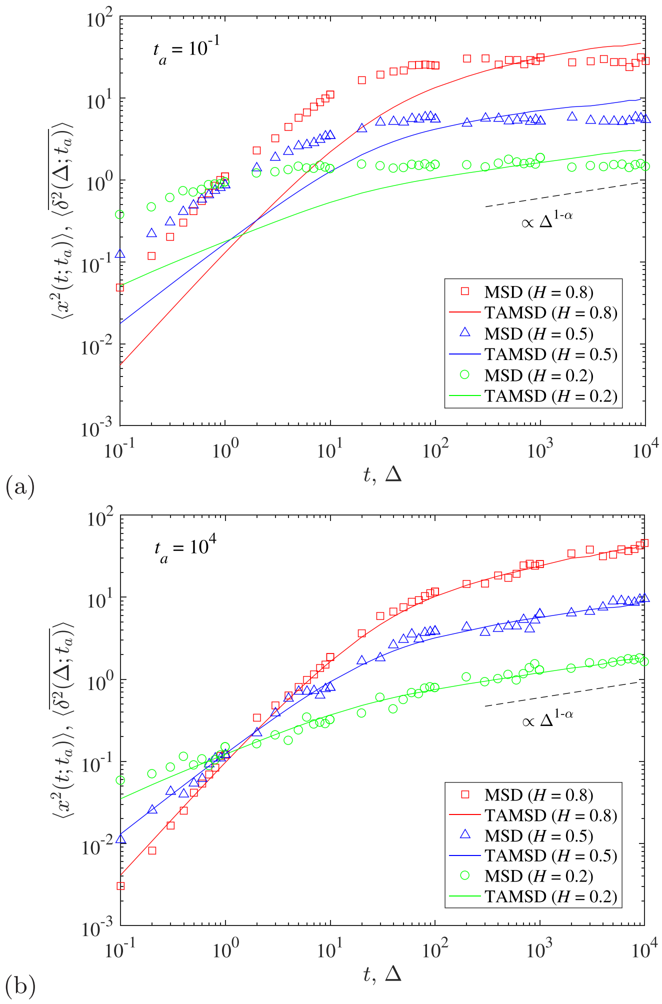

FIG. 9. Aged MSD and TAMSD of confined subordinated FBM for (a) $t_a = 10^{-1}$ and (b) $t_a = 10^4$. Parameters: $k = 0.1$, $\alpha = 0.8$, length of trajectories $T = 10^4$.

Interestingly, with the characteristic relationships between different regimes of measurement time and aging time, the current results provide a useful tool to probe the underlying stochastic mechanism for aged systems. And the actual age t_a of the system can be estimated based on the explicit results, which will be of interest in the analysis of systems without known age [97].

For confined subordinated FBM, at short times the MSD and TAMSD are the same as those for the free-subordinated FBM, while at long times the MSD quickly approaches a stationary value, contrasting the sublinear power-law increase in lag time of the TAMSD. Interestingly, the results of the MSD are similar to those of confined FBM and those of the TAMSD are similar to a confined CTRW. Short aging times t_a have no effect on the aged MSD, while at long aging times the aged MSD shows a power-law increase and is identical to the aged TAMSD.

We also note that the external force considered in the Langevin equation (21) in this study only influences the dynamical behavior at the instants of jumps, as proposed for the original CTRW process [37]. There, the traps are considered so deep that the external force does not affect the trapping-time statistic. In contrast, the force may keep acting on the system all the time, even when the particle is trapped as given in recent works [74,78,79] and the relevant Langevin equation is

$$\frac{dy(t)}{dt} = F(y(t)) + \bar{\zeta}_H(t), \tag{31}$$

where $\bar{\zeta}_H(t) = \int_0^{+\infty} \zeta_H(s)\delta[t - t(s)]ds$. Driven by the force $F(y) = -ky$, the process $y(t)$ is rapidly damped towards zero position when the particles are waiting for the next jump during long-trapping events. This effects a decrease of the MSD to zero at sufficiently long times $t \gg k^{-1}$ [79]. The mean TAMSDs will arrive at a plateau which is different from the MSD Eq. (26) and the TAMSD Eq. (27) of the process $x(t)$ with external force acting only on the jumps given by the Langevin equation (21).

The results reported here contribute to the development of aging and confined diffusion processes and can be used to detect the exact stochastic mechanism underlying experimental single-particle trajectories in complex systems. It will be important to include compound processes as the one studied here in efforts to identify the underlying stochastic process(es) and the associated parameters from data [105,106], such as by using classical observables [52,53] as well as Bayesian [107,108] or machine learning approaches [109–112]. In particular, the effect of static and dynamic noise should be studied for the subordinated FBM model [112].

ACKNOWLEDGMENTS

Y.L. acknowledges financial support from the Alexander von Humboldt Foundation (Grant No. 1217531) and the National Natural Science Foundation of China (Grant No. 12372382). R.M. acknowledges financial support from the German Science Foundation (DFG, Grant No. ME 1535/12-1).

[1] F. Höfling and T. Franosch, Anomalous transport in the crowded world of biological cells, Rep. Prog. Phys. **76**, 046602 (2013).

[2] K. Nørregaard, R. Metzler, C. Ritter, K. Berg-Sørensen, and L. Oddershede, Manipulation and motion of organelles and single molecules in living cells, Chem. Rev. **117**, 4342 (2017).

[3] A. Agrawal, Z. C. Scott, and E. F. Koslover, Morphology and transport in eukaryotic cells, Ann. Rev. Biphys. **51**, 247 (2022).

[4] E. Barkai, Y. Garini, and R. Metzler, Strange kinetics of single molecules in living cells, Phys. Today **65**(8), 29 (2012).

[5] D. Krapf and R. Metzler, Strange interfacial molecular dynamics, Phys. Today **72**(9), 48 (2019).

[6] Y. Meroz and I. M. Sokolov, A toolbox for determining subdiffusive mechanisms, Phys. Rep. **573**, 1 (2015).

[7] S. Yui, Y. Tang, W. Guo, H. Kobayashi, and M. Tsubota, Universal anomalous diffusion of quantized vortices in ultraquantum turbulence, Phys. Rev. Lett. **129**, 025301 (2022).

[8] Y. E. Litvinenko, H. Fichtner, and D. Walter, Anomalous transport of cosmic rays in a nonlinear diffusion model, Astrophys. J. **841**, 57 (2017).

[9] M. Weiss, M. Elsner, F. Karberg, and T. Nilsson, Anomalous subdiffusion is a measure for cytoplasmic crowding in living cells, Biophys. J. **87**, 3518 (2004).

[10] F. Etoc, E. Balloul, C. Vicario, D. Normanno, D. Lioe, A. Sittner, J. Piehler, M. Dahan, and M. Coppey, Non-specific interactions govern cytosolic diffusion of nanosized objects in mammalian cells, Nat. Mater. **17**, 740 (2018).

[11] H. Sun, M. Meerschaert, Y. Zhang, J. Zhu, and W. Chen, A fractal Richards' equation to capture the non-Boltzmann scaling of water transport in unsaturated media, Adv. Water Resour. **52**, 292 (2013).

[12] Y. Liang, S. Yan, P. Tian, and W. Xu, Characterization of solute mixing in heterogeneous media by means of fractal dilution index, Transp. Porous Med. **148**, 123 (2023).

[13] R. Metzler and J. Klafter, The random walk's guide to anomalous diffusion: A fractional dynamics approach, Phys. Rep. **339**, 1 (2000).

[14] I. M. Sokolov, Models of anomalous diffusion in crowded environments, Soft Matter **8**, 9043 (2012).

[15] R. Metzler, J.-H. Jeon, A. G. Cherstvy, and E. Barkai, Anomalous diffusion models and their properties: Non-stationarity, non-ergodicity, and ageing at the centenary of single particle tracking, Phys. Chem. Chem. Phys. **16**, 24128 (2014).

[16] I. Golding and E. C. Cox, Physical nature of bacterial cytoplasm, Phys. Rev. Lett. **96**, 098102 (2006).

[17] J.-H. Jeon, V. Tejedor, S. Burov, E. Barkai, C. Selhuber-Unkel, K. Berg-Sørensen, L. Oddershede, and R. Metzler, In vivo anomalous diffusion and weak ergodicity breaking of lipid granules, Phys. Rev. Lett. **106**, 048103 (2011).

[18] G. Guigas, C. Kalla, and M. Weiss, Probing the nanoscale viscoelasticity of intracellular fluids in living cells, Biophys. J. **93**, 316 (2007).

[19] A. Caspi, R. Granek, and M. Elbaum, Enhanced diffusion in active intracellular transport, Phys. Rev. Lett. **85**, 5655 (2000).

[20] W. He, H. Song, Y. Su, L. Geng, B. J. Ackerson, H. B. Peng, and P. Tong, Dynamic heterogeneity and non-Gaussian statistics for acetylcholine receptors on live cell membrane, Nat. Commun. **7**, 11701 (2016).

[21] S. Gupta, J. U. De Mel, R. M. Perera, P. Zolnierczuk, M. Bleuel, A. Faraone, and G. J. Schneider, Dynamics of phospholipid membranes beyond thermal undulations, J. Phys. Chem. Lett. **9**, 2956 (2018).

[22] J.-H. Jeon, H. Martinez-Seara Monne, M. Javanainen, and R. Metzler, Anomalous diffusion of phospholipids and cholesterols in a lipid bilayer and its origins, Phys. Rev. Lett. **109**, 188103 (2012).

[23] J.-H. Jeon, M. Javanainen, H. Martinez-Seara, R. Metzler, and I. Vattulainen, Protein crowding in lipid bilayers gives rise to non-Gaussian anomalous lateral diffusion of phospholipids and proteins, Phys. Rev. X **6**, 021006 (2016).

[24] A. V. Weigel, B. Simon, M. M. Tamkun, and D. Krapf, Ergodic and nonergodic processes coexist in the plasma membrane as observed by single-molecule tracking, Proc. Natl. Acad. Sci. USA **108**, 6438 (2011).

[25] S. S. Rogers, C. Van Der Walle, and T. A. Waigh, Microrheology of bacterial biofilms in vitro: Staphylococcus aureus and Pseudomonas aeruginosa, Langmuir **24**, 13549 (2008).

[26] Y. Liang, Q. Y. Allen, W. Chen, R. G. Gatto, L. Colon-Perez, T. H. Mareci, and R. L. Magin, A fractal derivative model for the characterization of anomalous diffusion in magnetic resonance imaging, Commun. Nonlinear Sci. **39**, 529 (2016).

[27] G. Seisenberger, M. U. Ried, T. Endreß, H. Büning, M. Hallek, and C. Bräuchle, Real-time single-molecule imaging of the infection pathway of an adeno-associated virus, Science **294**, 1929 (2001).

[28] M. S. Song, H. C. Moon, J.-H. Jeon, and H. Y. Park, Neuronal messenger ribonucleoprotein transport follows an aging Lévy walk, Nat. Commun. **9**, 344 (2018).

[29] J. F. Reverey, J.-H. Jeon, H. Bao, M. Leippe, R. Metzler, and C. Selhuber-Unkel, Superdiffusion dominates intracellular particle motion in the supercrowded space of pathogenic *Acanthamoeba castellanii*, Sci. Rep. **5**, 11690 (2015).

[30] A. G. Cherstvy, O. Nagel, C. Beta, and R. Metzler, Non-Gaussianity, population heterogeneity, and transient superdiffusion in the spreading dynamics of amoeboid cells, Phys. Chem. Chem. Phys. **20**, 23034 (2018).

[31] R. Großmann, L. S. Bort, T. Moldenhawer, M. Stange, S. S. Panah, R. Metzler, and C. Beta, Non-Gaussian displacements in active transport on a carpet of motile cells, Phys. Rev. Lett. **132**, 088301 (2024).

[32] M. de Jager, F. J. Weissing, P. M. Herman, B. A. Nolet, and J. van de Koppel, Lévy walks evolve through interaction between movement and environmental complexity, Science **332**, 1551 (2011).

[33] J. W. Kirchner, X. Feng, and C. Neal, Fractal stream chemistry and its implications for contaminant transport in catchments, Nature (London) **403**, 524 (2000); see also the discussion in H. Scher, G. Margolin, R. Metzler, J. Klafter, and B. Berkowitz, The dynamical foundation of fractal stream chemistry: The origin of extremely long retention times, Geophys. Res. Lett. **29**, 1061 (2002).

[34] A. Rajyaguru, R. Metzler, I. Dror, D. Grolimund, and B. Berkowitz, Diffusion in porous rock is anomalous, Environ. Sci. Technol. **58**, 8946 (2024).

[35] P. Tian and Y. Liang, Material coordinate driven variable-order fractal derivative model of water anomalous adsorption in swelling soil, Chaos Soliton. Fract. **164**, 112754 (2022).

[36] E. W. Montroll and G. H. Weiss, Random walks on lattices. II, J. Math. Phys. **6**, 167 (1965).

[37] H. Scher and E. W. Montroll, Anomalous transit-time dispersion in amorphous solids, Phys. Rev. B **12**, 2455 (1975).

[38] O. Rubner and A. Heuer, From elementary steps to structural relaxation: A continuous-time random-walk analysis of a supercooled liquid, Phys. Rev. E **78**, 011504 (2008).

[39] Y. Zhang, D. Zhou, M. Yin, H. Sun, W. Wei, S. Li, and C. Zheng, Nonlocal transport models for capturing solute transport in one-dimensional sand columns: Model review, applicability, limitations and improvement, Hydrol. Process. **34**, 5104 (2020).

[40] J. M. Berger and B. Mandelbrot, A new model for error clustering in telephone circuits, IBM J. **7**, 224 (1963).

[41] E. W. Montroll and H. Scher, Random walks on lattices. IV. Continuous-time walks and influence of absorbing boundaries, J. Stat. Phys. **9**, 101 (1973).

[42] M. F. Shlesinger, Asymptotic solutions of continuous-time random walks, J. Stat. Phys. **10**, 421 (1974).

[43] J.-P. Bouchaud and A. Georges, Anomalous diffusion in disordered media: Statistical mechanisms, models and physical applications, Phys. Rep. **195**, 127 (1990).

[44] B. D. Hughes, *Random Walks and Random Environments, Vol. I: Random Walks* (Oxford University Press, Oxford, UK, 1995).

[45] A. N. Kolmogorov, The local structure of turbulence in an incompressible fluid at very high Reynolds numbers, Dokl. Acad. Nauk USSR **30**, 299 (1940).

[46] B. B. Mandelbrot and J. W. van Ness, Fractional Brownian motions, fractional noises and applications, SIAM Rev. **10**, 422 (1968).

[47] J. Szymanski and M. Weiss, Elucidating the origin of anomalous diffusion in crowded fluids, Phys. Rev. Lett. **103**, 038102 (2009).

[48] J-.H. Jeon, N. Leijnse, L. Oddershede, and R. Metzler, Anomalous diffusion and power-law relaxation in wormlike micellar solution, New J. Phys. **15**, 045011 (2013).

[49] S. C. Weber, A. J. Spakowitz, and J. A. Theriot, Bacterial chromosomal loci move subdiffusively through a viscoelastic cytoplasm, Phys. Rev. Lett. **104**, 238102 (2010).

[50] S. Janušonis, N. Detering, R. Metzler, and T. Vojta, Serotonergic axons as fractional Brownian motion paths: Insights into the self-organization of regional densities, Front. Comput. Neurosci. **14**, 56 (2020).

[51] S. Rostek and R. Schöbel, A note on the use of fractional Brownian motion for financial modeling, Econ. Model. **30**, 30 (2013).

[52] O. Vilk, E. Aghion, T. Avgar, C. Beta, O. Nagel, A. Sabri, R. Sarfati, D. K. Schwartz, M. Weiss, D. Krapf, R. Nathan, R. Metzler, and M. Assaf, Unravelling the origins of anomalous diffusion: from molecules to migrating storks, Phys. Rev. Res. **4**, 033055 (2022).

[53] O. Vilk, E. Aghion, R. Nathan, S. Toledo, R. Metzler, and M. Assaf, Classification of anomalous diffusion in animal movement data using power spectral analysis, J. Phys. A **55**, 334004 (2022).

[54] A. Sabri, X. Xu, D. Krapf, and M. Weiss, Elucidating the origin of heterogeneous anomalous diffusion in the cytoplasm of mammalian cells, Phys. Rev. Lett. **125**, 058101 (2020).

[55] S. Scott, M. Weiss, C. Selhuber-Unkel, Y. F. Barooji, A. Sabri, J. T. Erler, R. Metzler, and L. B. Oddershede, Extracting, quantifying, and comparing dynamical and biomechanical properties of living matter through single particle tracking, Phys. Chem. Chem. Phys. **25**, 1513 (2023).

[56] C. Ayaz, L. Tepper, F. N. Brünig, J. Kappler, J. O. Daldrop, and R. R. Netz, Non-Markovian modeling of protein folding, Proc. Natl. Acad. Sci. U S A **118**, e2023856118 (2021).

[57] N. A. Bustos, C. M. Saad-Roy, A. G. Cherstvy, and C. E. Wagner, Distributed medium viscosity yields quasi-exponential step-size probability distributions in heterogeneous media, Soft Matter **18**, 8572 (2022).

[58] A. Díez Fernandez, P. Charchar, A. G. Cherstvy, R. Metzler, and M. W. Finnis, The diffusion of doxorubicin drug molecules in silica nanochannels is non-Gaussian and intermittent, Phys. Chem. Chem. Phys. **22**, 27955 (2020).

[59] S. M. A. Tabei, S. Burov, H. Y. Kima, A. Kuznetsov, T. Huynh, J. Jureller, L. H. Philipson, A. R. Dinner, and N. F. Scherer, Intracellular transport of insulin granules is a subordinated random walk, Proc. Natl. Acad. Sci. USA **110**, 4911 (2013).

[60] A. Mosqueira, P. A. Camino, and F. J. Barrantes, Cholesterol modulates acetylcholine receptor diffusion by tuning confinement sojourns and nanocluster stability, Sci. Rep. **8**, 11974 (2018).

[61] Z. R. Fox, E. Barkai, and D. Krapf, Aging power spectrum of membrane protein transport and other subordinated random walks, Nat. Commun. **12**, 6162 (2021).

[62] S. Bochner, Subordination of non-Gaussian stochastic processes, Proc. Natl. Acad. Sci. USA **48**, 19 (1962).

[63] A. Chechkin and I. M. Sokolov, Relation between generalized diffusion equations and subordination schemes, Phys. Rev. E **103**, 032133 (2021).

[64] W. Feller, *An Introduction to Probability Theory and its Applications* (Wiley, New York Wiley, 1971).

[65] Y. Liang, W. Wang, and R. Metzler, Anomalous diffusion, non-Gaussianity, and nonergodicity for subordinated fractional Brownian motion with a drift, Phys. Rev. E **108**, 024143 (2023).

[66] J. Rottler and M. O. Robbins, Unified description of aging and rate effects in yield of glassy solids, Phys. Rev. Lett. **95**, 225504 (2005).

[67] M. Schubert, E. Preis, J. C. Blakesley, P. Pingel, U. Scherf, and D. Neher, Mobility relaxation and electron trapping in a donor/acceptor copolymer, Phys. Rev. B **87**, 024203 (2013).

[68] X. Brokmann, J. P. Hermier, G. Messin, P. Desbiolles, J. P. Bouchaud, and M. Dahan, Statistical aging and nonergodicity in the fluorescence of single nanocrystals, Phys. Rev. Lett. **90**, 120601 (2003).

[69] E. Barkai, and Y. C. Cheng, Aging continuous time random walks, J. Chem. Phys. **118**, 6167 (2003).

[70] J.-H. Jeon and R. Metzler, Inequivalence of time and ensemble averages in ergodic systems: Exponential versus power-law relaxation in confinement, Phys. Rev. E **85**, 021147 (2012).

[71] P. Meyer and R. Metzler, Stochastic processes in a confining harmonic potential in the presence of static and dynamic measurement noise, New J. Phys. **25**, 063003 (2023).

[72] T. Guggenberger, A. V. Chechkin, and R. Metzler, Fractional Brownian motion in superharmonic potentials and non-Boltzmann stationary distributions, J. Phys. A: Math. Theor. **54**, 29LT01 (2021).

[73] S. Burov, R. Metzler, and E. Barkai, Aging and nonergodicity beyond the Khinchin theorem, Proc. Natl. Acad. Sci. USA **107**, 13228 (2010).

[74] M. Magdziarz, R. Metzler, W. Szczotka, and P. Zebrowski, Correlated continuous-time random walks in external force fields, Phys. Rev. E **85**, 051103 (2012).

[75] J. Kursawe, J. H. P. Schulz, and R. Metzler, Transient ageing in fractional Brownian and Langevin equation motion, Phys. Rev. E **88**, 062124 (2013).

[76] S. Burov and E. Barkai, Fractional Langevin equation: Overdamped, underdamped, and critical behaviors, Phys. Rev. E **78**, 031112 (2008).

[77] R. Metzler, E. Barkai, and J. Klafter, Anomalous diffusion and relaxation close to thermal equilibrium: A fractional Fokker-Planck equation approach, Phys. Rev. Lett. **82**, 3563 (1999).

[78] Y. Chen, X. Wang, and W. Deng, Subdiffusion in an external force field, Phys. Rev. E **99**, 042125 (2019).

[79] A. Cairoli and A. Baule, Langevin formulation of a subdiffusive continuous-time random walk in physical time, Phys. Rev. E **92**, 012102 (2015).

[80] H. C. Fogedby, Langevin equations for continuous time Lévy flights, Phys. Rev. E **50**, 1657 (1994).
[81] D. Kleinhans and R. Friedrich, Continuous-time random walks: Simulation of continuous trajectories, Phys. Rev. E **76**, 061102 (2007).
[82] Y. Zhang, M. M. Meerschaert, and B. Baeumer, Particle tracking for time-fractional diffusion, Phys. Rev. E **78**, 036705 (2008).
[83] R. Gorenflo and F. Mainardi, Subordination pathways to fractional diffusion, Eur. Phys. J. Spec. Top. **193**, 119 (2011).
[84] M. Magdziarz, A. Weron, and J. Klafter, Equivalence of the fractional Fokker-Planck and subordinated Langevin equations: The case of a time-dependent force, Phys. Rev. Lett. **101**, 210601 (2008).
[85] K. A. Penson and K. Górska, Exact and explicit probability densities for one-sided Lévy stable distributions, Phys. Rev. Lett. **105**, 210604 (2010).
[86] K. A. Penson and K. Górska, On the properties of Laplace transform originating from one-sided Lévy stable laws, J. Phys. A: Math. Theor. **49**, 065201 (2016).
[87] M. M. Meerschaert and P. Straka, Inverse stable subordinators, Math. Model. Nat. Phenom. **8**, 1 (2013).
[88] A. Compte, R. Metzler, and J. Camacho, Biased continuous time random walks between parallel plates, Phys. Rev. E **56**, 1445 (1997).
[89] H. Krüsemann, A. Godec, and R. Metzler, Ageing first passage time density in continuous time random walks and quenched energy landscapes, J. Phys. A **48**, 285001 (2015).
[90] M. Abramowitz and I. A. Stegun, Editors, Handbook of mathematical functions with formulas, graphs, and mathematical tables National Bureau of Standards Applied Mathematics Series **55**, June 1964.
[91] Y. He, S. Burov, R. Metzler, and E. Barkai, Random time-scale invariant diffusion and transport coefficients, Phys. Rev. Lett. **101**, 058101 (2008).
[92] J. H. P. Schulz, E. Barkai, and R. Metzler, Aging effects and population splitting in single-particle trajectory averages, Phys. Rev. Lett. **110**, 020602 (2013).
[93] J. H. P. Schulz, E. Barkai, and R. Metzler, Aging renewal theory and application to random walks, Phys. Rev. X **4**, 011028 (2014).
[94] W. Deng and E. Barkai, Ergodic properties of fractional Brownian-Langevin motion, Phys. Rev. E **79**, 011112 (2009).
[95] H. Safdari, A. V. Chechkin, G. R. Jafari, and R. Metzler, Aging scaled Brownian motion, Phys. Rev. E **91**, 042107 (2015).
[96] A. G. Cherstvy, A. V. Chechkin, and R. Metzler, Ageing and confinement in non-ergodic heterogeneous diffusion processes, J. Phys. A: Math. Theor. **47**, 485002 (2014).
[97] H. Krüsemann, A. Godec, and R. Metzler, First-passage statistics for aging diffusion in systems with annealed and quenched disorder, Phys. Rev. E **89**, 040101(R) (2014).
[98] L. Huang, P. Yan, and Y. Liu, Effect of alkali content in cement on the fluidity and structural build-up of plasticized cement pastes, Constr. Build. Mater. **253**, 119180 (2020).
[99] M. A. Chaudhry and S. M. Zubair, *On a Class of Incomplete Gamma Functions with Applications* (Chapman & Hall/CRC, London, UK, 2001).
[100] A. Gil, J. Segura, and N. M. Temme, Computing the Kummer function $U(a, b, z)$ for small values of the arguments, Appl. Math. Comput. **271**, 532 (2015).
[101] A. Erdélyi, Editor, *Higher Transcendental Functions, Vol. III: Bateman Manuscript Project* (Robert E. Krieger Publishing Company, Malabar, FL, 1953).
[102] Yu. L. Klimontovich, *Turbulent Motion and the Structure of Chaos: A New Approach to the Statistical Theory of Open Systems* (Kluwer, Dordrecht, Netherlands, 1992).
[103] O. Yu. Sliusarenko, V. Yu. Gonchar, A. V. Chechkin, I. M. Sokolov, and R. Metzler, Kramers escape driven by fractional Brownian motion, Phys. Rev. E **81**, 041119 (2010).
[104] T. Neusius, I. M. Sokolov, and J. C. Smith, Subdiffusion in time-averaged, confined random walks, Phys. Rev. E **80**, 011109 (2009).
[105] G. Muñoz-Gil, G. Volpe, M. A. Garcia-March, E. Aghion, A. Argun, C. B. Hong, T. Bland, S. Bo, J. A. Conejero, N. Firbas, Ò. Garibo i Orts, A. Gentili, Z. Huang, J.-H. Jeon, H. Kabbech, Y. Kim, P. Kowalek, D. Krapf, H. Loch-Olszewska, M. A. Lomholt, J.-B. Masson *et al.*, Objective comparison of methods to decode anomalous diffusion, Nat. Commun. **12**, 6253 (2021).
[106] G. Muñoz-Gil, H. Bachimanchi, J. Pineda, B. Midtvedt, M. Lewenstein, R. Metzler, D. Krapf, G. Volpe, and C. Manzo, Quantitative evaluation of methods to analyze motion changes in single-particle experiments, arXiv:2311.18100.
[107] J. Krog, L. H. Jacobsen, F. W. Lund, D. Wüstner, and M. A. Lomholt, Bayesian model selection with fractional Brownian motion, J. Stat. Mech. (2018) 093501.
[108] S. Thapa, M. A. Lomholt, J. Krog, A. G. Cherstvy, and R. Metzler, Bayesian nested sampling analysis of single particle tracking data: Maximum likelihood model selection applied to stochastic diffusivity data, Phys. Chem. Chem. Phys. **20**, 29018 (2018).
[109] G. Muñoz-Gil, M. A. Garcia-March, C. Manzo, J. D. Martín-Guerrero, and M. Lewenstein, Single trajectory characterization via machine learning, New J. Phys. **22**, 013010 (2020).
[110] H. Seckler and R. Metzler, Bayesian deep learning for error estimation in the analysis of anomalous diffusion, Nat. Commun. **13**, 6717 (2022).
[111] H. Loch-Olszewska and J. Szwabiński, Impact of feature choice on machine learning classification of fractional anomalous diffusion, Entropy **22**, 1436 (2020).
[112] H. Seckler, J. Szwabiński, and R. Metzler, Machine-learning solutions for the analysis of single-particle diffusion trajectories, J. Phys. Chem. Lett. **14**, 7910 (2023).